

Original Article

A pilot study in epilepsy patients using simultaneous PET/MR

Yu-Shin Ding^{1,2}, Bang-Bin Chen³, Christopher Glielmi⁴, Kent Friedman¹, Orrin Devinsky⁵

Departments of ¹Radiology, ²Psychiatry, ⁵Neurology, New York University School of Medicine, New York, NY, USA; ³Medical College and Hospital, National Taiwan University, Taipei, Taiwan; ⁴Siemens Healthcare, New York, NY

Received April 27, 2014; Accepted May 27, 2014; Epub August 15, 2014; Published August 30, 2014

Abstract: Integrated PET/MR with simultaneous acquisition may improve the identification of pathologic findings in patients. This pilot study evaluated metabolic activity differences between epilepsy patients and healthy controls and directly correlated FDG uptake with MR regional abnormality. Epilepsy patients (n=11) and controls (n=6) were imaged on a whole-body simultaneous PET/MR scanner. After FDG injection, simultaneous images were acquired for 60 minutes. Statistical analyses on SUV values (over 117 brain regions, including left and right, for 96 cortical and 21 subcortical regions) derived from three normalization methods, by individual subject's mean cortical, white matter or global brain, were compared between groups. The asymmetry was compared. T2, T1 and PET co-registered images were also used for lesion detection and correlation of PET and MR regional abnormality. Left and right postcentral gyri were found to be consistently hypermetabolic regions, while right temporal pole and planum polare were consistently hypometabolic regions by all three normalization methods. Using the asymmetry index (AI > 10% or SUV ratios > 1.2), more metabolic asymmetry regions were detected in patients than in controls, with 96.2% agreement. The presence of hippocampal abnormalities or cortical tubers detected via T2 FLAIR in patients correlated well with the hypometabolism detected via FDG-PET. Our results showed specific patterns of metabolic abnormality and asymmetry over 117 brain regions in epilepsy patients, as compared to controls, suggest that simultaneous PET/MR imaging provides a useful tool to help understand etiopathogenesis and localize seizure foci.

Keywords: Epilepsy, simultaneous PET/MR, FDG, asymmetry, hypermetabolism, hypometabolism

Introduction

Epilepsy is one of the most common neurologic disorders, affecting 0.5-1% of the population [1]. Early detection of epileptogenic regions could help presurgical evaluation and seizure control. Radionuclide imaging, such as positron emission tomography (PET), can demonstrate metabolic or functional abnormality especially in cases when structural imaging (CT or MR) is normal or equivocal. MR imaging may detect subtle or major malformations associated with seizures, which may not be associated with an obvious metabolic abnormality. Recently developed integrated PET/MR may improve the characterization of pathologic findings by combining the simultaneously acquired MR and PET images. The high resolution of MRI can be utilized for the attenuation correction [2] and motion correction [3], and help to quantify PET data, e.g., arterial input function can be derived via

MRI methods without blood sampling [4]. Integrated PET/MR holds great potential for brain research, especially for multi-parametric analysis of functional neuronal networks in epilepsy patients. Image fusion can also be valuable in the presurgical evaluation for epilepsy surgery.

[¹⁸F]fluorodeoxyglucose (FDG) PET can often detect interictal seizure foci as areas of focally reduced regional cerebral metabolic rate for glucose [5]. Focal cortical abnormalities of neuronal architecture may be associated with interictal hypometabolism on FDG-PET scans [6, 7]. FDG-PET may also help to assess the integrity of the regions remote from focal abnormalities [8].

Although areas affected in epilepsy patients differ in their anatomical distribution, it may be necessary to run a normalization procedure in

Table 1. Subject characteristics for healthy controls (HC) and patients (Pt)

Group	Age	Gender	Diagnosis (Epileptic side)
HC01	36	F	NA
HC02	24	M	NA
HC03	24	M	NA
HC04	28	M	NA
HC05	20	M	NA
HC06	23	F	NA
Pt01	24	F	Left
Pt02	32	M	Right
Pt03	32	F	Bilateral
Pt04	58	M	TSC; seizure localization uncertain
Pt05	46	F	Bilateral
Pt06	17	M	Right
Pt07	60	M	Right
Pt08	52	M	Bilateral
Pt09	9	F	Left
Pt10	10	F	Right
Pt11	24	F	Left

NA: not applicable; TSC: tuberous sclerosis complex.

order to compare the relative regional metabolic rate within subjects, within a group, or between groups. This procedure removes inter-subject differences in the absolute whole brain intensity by relativizing the absolute glucose metabolic rate in the whole brain to a reference area. For example, different amounts of a radiopharmaceutical or a contrast agent injected may result in inter-subject differences. Specific regional uptake can be expressed as a ratio of the uptake against a reference such as whole brain [9], white matter, or cortical area [10], to assist the detection of focal, bilateral and diffuse cortical defects. At present, there is no consensus as to which reference region should be used. Focal cortical abnormalities can also be detected by comparing radiotracer uptake in regions of interest (ROIs) placed in homologous brain regions. This can be quantified by calculating asymmetry indices (AI).

PET and MRI co-registration images may be suboptimal to detect seizure foci since these two images were performed in different machines and at different times. Misregistration or various motion artifacts may introduce errors [11]. A combined PET/MR scanner with simultaneous acquisition permits simultaneous imaging of physiologic and pathophysiologic processes and provides both anatomical and

functional information on the same subject. It allows direct correlations of PET data with MR-detected patterns of neural synchrony in both grey and white matters; e.g., resting-state fMRI, diffusional kurtosis imaging, and MRS. This multi-modal analysis will facilitate the identification of an optimal biomarker. To demonstrate feasibility of this, we initiated a pilot study using FDG in patients with epilepsy, and compared to healthy controls. In this preliminary report, quantitative data analysis on glucose metabolism in ~120 brain regions was compared between two groups using three normalization methods (i.e., with means of cortical area, deep white matter or global brain, as a reference). Subject asymmetry was accessed via asymmetry indices. Direct correlations of FDG uptake to MR findings for specific regional abnormality in patients were also presented.

Material and methods

Patients and control subjects

We examined 17 subjects in this study (**Table 1**; eleven patients (6F, mean age 33) had epilepsy and were considered potential surgical candidates at the New York University (NYU) Epilepsy Center). Diagnostic evaluation was performed following the standard presurgical evaluation, which also included clinical, neuropsychological, and video-EEG studies. Seizure focus lateralization/localization of patients was made by epileptologists based on clinical criteria including neuroimaging, video-EEG, and intracranial EEG (iEEG) when available. We excluded patients with grossly structural distorted MRI that could interfere with image processing, serious medical/neurologic disease other than epilepsy, or serious psychiatric disease such as psychosis. For comparison, six healthy controls (HC) were recruited (2F, avg. age 26, respectively). The research protocol was approved by the ethics committee of the New York University Medical Center.

All subjects were free of serious medical or non-epilepsy neurological disorders such as dementia, cancer, cardiovascular, endocrine, renal, liver, or thyroid pathology. Exclusion criteria included pregnancy/breast feeding, urine positive for drugs with abuse liability, current psychiatric treatment for disorders such as depression and bipolar disease, regular use of

Study in epilepsy using simultaneous PET/MR

any psychotropic drugs, and MRI-incompatible implants and other contraindications for MRI.

PET/MR protocol

All examinations were performed using an integrated PET/MR system (Biograph, Siemens Healthcare), which allows for simultaneous acquisition of PET and MR of the brain. The system consists of an MR-compatible PET system inserted into a modified whole-body MR scanner at a field-strength of 3 T. The PET scanner has an axial field of view (FOV) of 19.25 cm. A standard birdcage transmit/receive head coil with an additional eight-channel receive-only coil inside was used for all examinations. After 6 h of fasting and blood-sugar surveillance, a bolus of FDG (185-310 MBq) was injected intravenously (max. injected dose: 10 mCi. For subjects < 18 yrs, dose was adjusted by weight, 0.1 mCi/kg). All image data were acquired in a listmode; all information for each coincidence event (e.g., timing and detector locations) was stored on a hard disk during the scan for retrospective data histogramming and reconstruction. After the scan all coincidence data were sorted into a 3D PET sinogram, which were subsequently reconstructed using an iterative 3D-OP-POSEM algorithm with 3 iterations and 21 subsets, or a Fourier rebinning of the 3D sinogram data followed by a 2D FBP reconstruction. Dixon sequence was acquired to obtain a μ -map for attenuation correction (AC) of PET data. The image volume consists of 127 transaxial image planes with a matrix size of 2 mm \times 2 mm \times 2 mm.

During PET data acquisition (for approx. 60 min), standard MR clinical pulse sequences were acquired as follows: a transversal 2D-encoded fluid attenuated inversion recovery (FLAIR) sequence (TR/TE, 9000/89; echo train length, 21; inversion time, 2.5 s; matrix size, 512 \times 512; in-plane resolution, 0.5 mm \times 0.5 mm; slice thickness, 3.5 mm; and bandwidth, 287 Hz/pixel); and sagittal 3D-encoded magnetization-prepared rapid-acquisition gradient-echo (MPRAGE) sequence (TR/TE, 1360/2.19; TI, 0.8 s; matrix size, 256 \times 256 \times 160; resolution, 1 mm \times 1 mm \times 1 mm; bandwidth, 199 Hz/pixel).

Post-processing by FSL

All MRI and PET DICOM images were converted to Nifti format using the software Mango

(<http://ric.uthscsa.edu/mango/>). The image data were preprocessed using MATLAB7.6 to obtain SUV (standardized uptake value)-coded PET images. SUV is defined as the ratio of the average radioactivity concentration obtained for each region to the injected dose per subject weight.

The summed SUV-coded FDG-PET images were registered to the individual subject's high-resolution T1 structural images, which, in turn, was registered to a 2 mm resolution standard MNI152 (Montreal Neurological Institute, Montreal, Québec, Canada) template by using an image registration tool (FLIRT, FMRIB's linear image registration tool; University of Oxford, www.fmrib.ox.ac.uk/fsl/flirt/index.html) via a 12-parameter rigid registration using normalized mutual information in FSL.

In FSL, all the atlases are registered to the MNI 152 model. The HarvardOxford Probabilistic atlas covers 96 cortical and 21 subcortical structural areas, derived from structural data and segmentations provided by the Harvard Center for Morphometric Analysis [12]. The regions of interest (ROI) identified by the Harvard-Oxford Atlas were used to create 117 masks and the mean SUV value for each mask was then calculated.

For direct correlation of FDG uptake with MR findings in patients, the FDG-PET images of selected cases were registered to the subject's own T2 FLAIR MR images by using FLIRT via a 12-parameter rigid registration using normalized mutual information in FSL. The lesions of abnormal signal detected by T2 FLAIR were manually drawn as ROIs and applied to the same areas on the PET-T2 co-registered images. The ROIs of contralateral homologous regions were used as reference. The SUVs of the lesion ROIs and the contralateral ROIs on PET images were compared.

Compare healthy controls and epilepsy patients using three normalization reference methods

Scans from epilepsy patients and healthy control subjects were compared to detect abnormality regions using quantitative analysis. Three normalization methods were evaluated; that is, the mean SUV value of each region was normalized by dividing by the whole-brain mean

Study in epilepsy using simultaneous PET/MR

Table 2. Comparison of metabolic activity between epilepsy patients and healthy controls in 117 brain regions using three normalization methods

Metabolism	SUV _{WM_norm}	<i>p</i>	SUV _{COR_norm}	<i>p</i>	SUV _{global_norm}	<i>p</i>
Pt > HC	L-Postcentral Gyrus (Mask33)	0.027	L-Postcentral Gyrus (Mask33)	0.035	L-Postcentral Gyrus (Mask33)	0.044
Pt > HC	R-Postcentral Gyrus (Mask34)	0.016	R-Postcentral Gyrus (Mask34)	0.016	R-Postcentral Gyrus (Mask34)	0.047
Pt > HC	R-Middle Frontal Gyrus (Mask8)	0.044	R-Middle Frontal Gyrus (Mask8)	0.044		
Pt > HC	R-Precentral Gyrus (Mask14)	0.012	R-Precentral Gyrus (Mask14)	0.035		
Pt > HC	L-Superior Parietal Lobule (Mask35)	0.012	L-Superior Parietal Lobule (Mask35)	0.035		
Pt > HC	L_Precentral Gyrus (Mask13)	0.044				
Pt < HC	R-Temporal Pole (Mask16)	0.044	R-Temporal Pole (Mask16)	0.035	R-Temporal Pole (Mask16)	0.035
Pt < HC	L-Planum Polare (Mask87)	0.016	L-Planum Polare (Mask87)	0.009	L-Planum Polare (Mask87)	0.007
			R-Insular Cortex (Mask4)	0.016	R-Insular Cortex (Mask4)	0.021
			L-Temporal Fusiform Cortex, anterior (Mask73)	0.035	L-Temporal Fusiform Cortex, anterior (Mask73)	0.035
					L-Insular Cortex (Mask3)	0.044

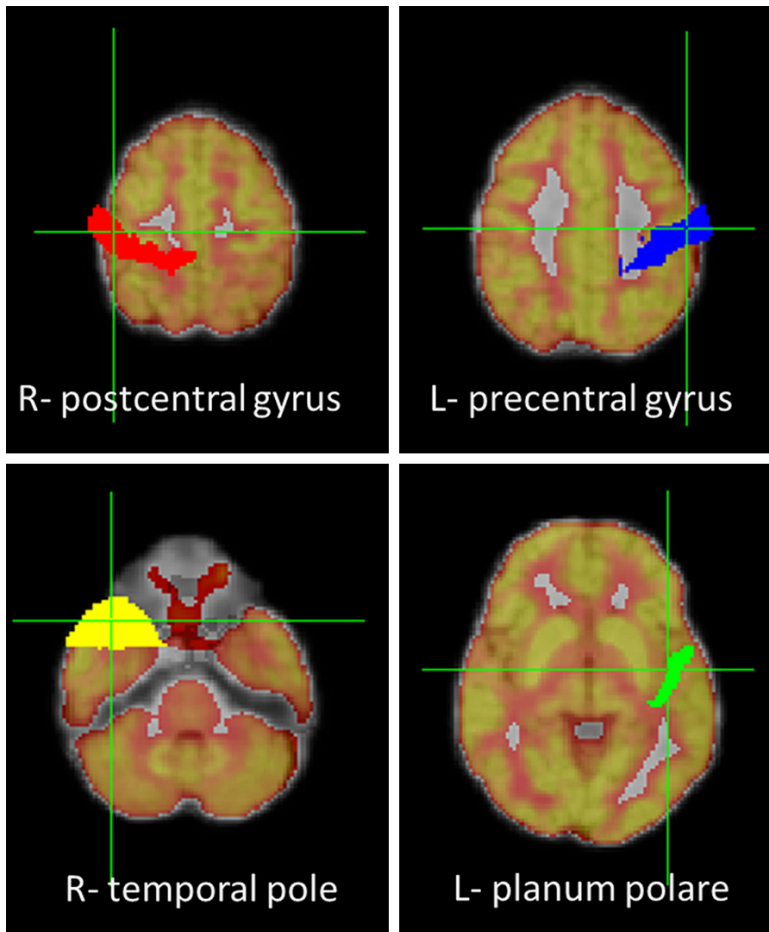


Figure 1. On the FDG-PET and MRI co-registered images, the upper row depicts the masks of right postcentral (red) and left precentral gyri (blue) that show hypermetabolism in epilepsy patients. The lower row depicts the masks of right temporal pole (yellow) and left planum polare (green) that show hypometabolism in epilepsy patients.

value (SUV_{global_norm}), or by the mean value of all cortical regions (SUV_{COR_norm}), or by the deep white matter value (SUV_{WM_norm}). The SUV_{global_norm} value for each subject was calculated from a ROI that includes whole brain (excluding air) generated in Mango with threshold mask > 1 from the SUV-coded brain images as described above. The SUV_{COR_norm} was the mean SUV values of all cortical masks (masks 1-96 based on HarvardOxford Probabilistic atlas) and the SUV_{WM_norm} was calculated from the deep white matter regions within the cerebellum based on HarvardOxford Probabilistic atlas. The normalized SUV values were then compared over the same anatomical areas between healthy controls and epilepsy patients. The SUV differences between right and left homologous brain regions were also compared using these three normalization methods.

Compare asymmetry in healthy controls and epilepsy patients using asymmetry index and SUV ratios

An asymmetry index [13, 14] (AI, used for detection of left-right asymmetries in neurodegenerative diseases) within each dataset was calculated for PET datasets based on the following equation: (mean value right ROIs - mean value left ROIs)/(mean value right ROIs + mean value left ROIs)*100, given in percent. Adult studies consider that an asymmetry of homologous cortical regions of 10~15% is abnormal [15, 16]. SUV ratios were calculated by dividing the SUV of the ipsilateral ROI by that of the contralateral homotopic ROI. A SUV ratio of ≥ 1.10 (i.e., $\geq 10\%$) was considered glucose hypermetabolism [17].

We evaluated the sensitivity of AI and SUV ratios in detecting metabolic asymmetry in all subjects, using $AI > 10\%$ and SUV ratios (≥ 1.10 or > 1.2) as the asymmetry thresholds.

Statistical analysis

Values were reported as mean \pm standard deviation. The Mann-Whitney U test and Wilcoxon sign rank test were performed to evaluate the differences in normalized SUV between healthy controls and epilepsy patients. P value < 0.05 was considered significant. SPSS (version 17.0; SPSS Inc.) was used for the data analyses.

Results

Compare metabolic activities in epilepsy patients and healthy controls using three normalization methods

Based on the statistical analyses on 117 brain regions examined, hypermetabolism in patients as compared to controls (Pt $>$ HC) were detect-

Study in epilepsy using simultaneous PET/MR

Table 3. Comparison of asymmetric index and SUV ratios in detecting metabolic asymmetry

Area	AI > 10%	SUV ratios > 1.2
L-Temporal Pole (Mask15)	-	Pt09
L-Superior Temporal Gyrus, posterior division (Mask19)	Pt04	Pt04
L-Middle Temporal Gyrus, anterior division (Mask21)	Pt04	Pt04
L-Middle Temporal Gyrus, posterior division (Mask23)	-	Pt04
L-Inferior Temporal Gyrus, anterior division (Mask27)	HC04, Pt04, Pt09	HC04, Pt04, Pt09
L-Intracalcarine Cortex (Mask47)	Pt09	Pt09
L-Temporal Fusiform Cortex, anterior division (Mask73)	-	Pt06
L-Planum Polare (Mask87)	Pt04	Pt04
L-Supracalcarine Cortex (Mask93)	Pt09	Pt09
L-Cerebral Cortex (Mask202)	Pt04, Pt08	Pt04, Pt08
L-Lateral Ventricle (Mask203)	Pt08	Pt08
L-Thalamus (Mask204)	Pt04	Pt04
L-Pallidum (Mask207)	HC01~06, Pt01~12	HC01~06, Pt01~12
L-Accumbens (Mask211)	Pt07	Pt02, Pt07

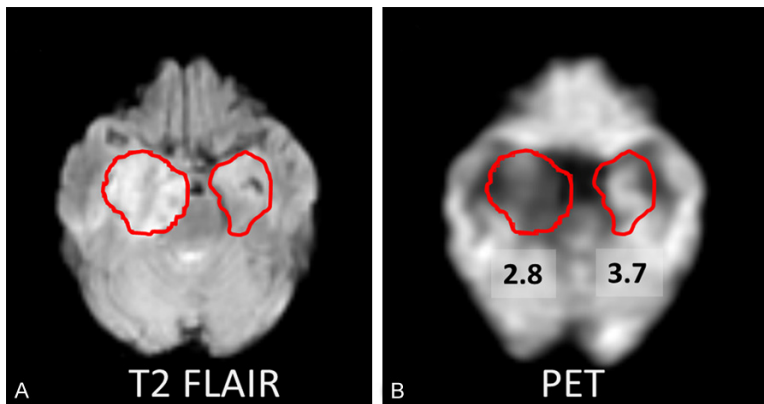


Figure 2. A: A 60-year-old male patient (case 7) shows abnormal signal and enlargement in right medial temporal lobe on T2 FLAIR image, as compared to the contralateral ROI. B: The co-registered FDG-PET and MRI image shows that this lesion has lower SUV (SUV=2.8) than contralateral homologous cortical region (SUV=3.7).

ed in 6 regions with SUV_{WM_norm} , 5 regions with SUV_{COR_norm} , and 2 regions with SUV_{global_norm} , as the normalization method (Table 2). Left and right postcentral gyri were consistently detected as hypermetabolic regions by all three normalization methods (Figure 1).

Hypometabolism in patients as compared to controls (Pt < HC) were detected in 2 regions with SUV_{WM_norm} , 4 regions with SUV_{COR_norm} , and 5 regions with SUV_{global_norm} . Right temporal pole and planum polare (anterior portion of the superior surface of the temporal lobe) were consistently detected as hypometabolic regions by all three normalization methods (the locations of these four ROIs, two hyper- & two hypo-

metabolism regions, are shown in Figure 1).

Compare asymmetry in healthy controls and epilepsy patients with asymmetry index and SUV ratios

Regarding metabolic asymmetry detection on a regional basis, epilepsy patients had more regions of metabolic asymmetry than healthy subjects. Based on the analysis of the overall pool of 106 regions, the AI > 10% and/or SUV ratios > 1.2 detected 14 (13%) asymmetric brain regions ($SUV_{right} > SUV_{left}$). Only 4 regions in 4 patients were dis-

cordant (Table 3), suggesting an overall weighted agreement of 96.2%.

When SUV ratio threshold was set as > 1.1, additional metabolic asymmetric regions (23 regions) were detected compared to the threshold 1.2, suggesting that SUV ratios > 1.1 might be more sensitive but less concordant with AI > 10% in detecting hypometabolism areas.

Direct correlation of FDG uptake with MR findings on selected cases

A 60-year-old male patient (case 7) showed abnormal signal and enlargement in right medial temporal lobe on T2 FLAIR image. The co-

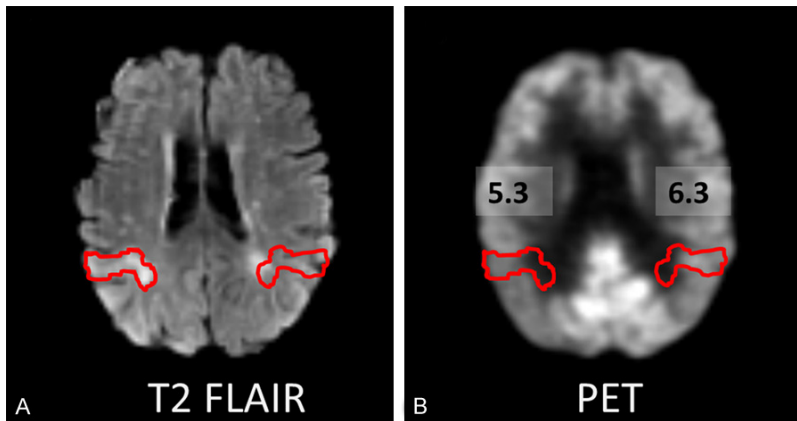


Figure 3. A: A 58-year-old male patient (case 4) with tuberous sclerosis shows an abnormal cortical tuber in right parietal lobe on T2 FLAIR image. B: The co-registered FDG-PET and MRI image shows that this lesion has lower SUV (SUV=5.3) than contralateral homologous cortical region (SUV=6.3).

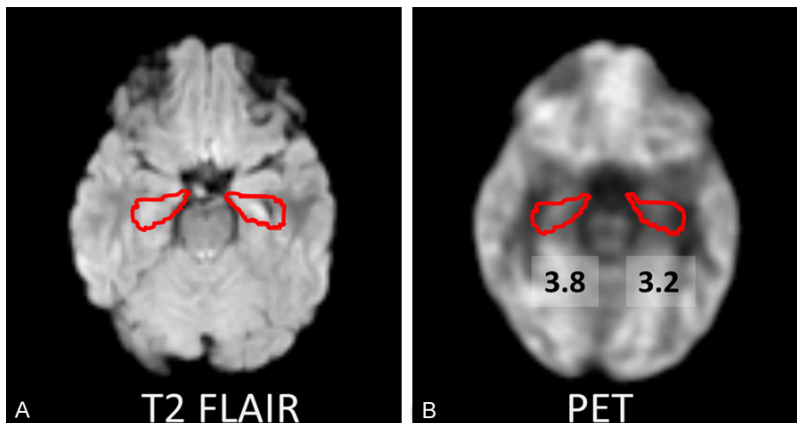


Figure 4. A: A 9-year-old female patient (case 9) with left hippocampal sclerosis shows slightly atrophy of left hippocampus on T2 FLAIR image. B: The co-registered FDG-PET and MRI image shows that left hippocampus has lower SUV (SUV=3.2) than right hippocampus (SUV=3.8).

registered PET image confirmed that a lower SUV for the lesion area than that of the contralateral homologous cortical region (**Figure 2**).

A 58-year-old male patient (case 4) with tuberous sclerosis complex (TSC) showed an abnormal cortical tuber in right parietal lobe on T2 FLAIR image. TSC is a genetic disorder and 80-90% of TSC patients suffer with epilepsy, the most prevalent and disabling clinical manifestation of TSC and can be medically refractory [18-20]. The co-registered PET image demonstrated a lower SUV for the tuber than the contralateral homologous cortical region (**Figure 3**), consistent with previous studies showing hypometabolism in TSC tubers [21].

A 9-year-old female patient (case 9) with left hippocampal sclerosis showed slightly atrophy of left hippocampus on T2 FLAIR image. The co-registered PET image showed that the left hippocampus had lower SUV than right hippocampus (**Figure 4**).

Discussion

Our study examined the PET activity differences between epilepsy patients and healthy controls using a quantitative approach for different brain regions by simultaneously acquired and coregistered PET/MR. By using three normalization methods, the hypermetabolic regions in patients were consistently detected in the both postcentral gyri, and hypometabolic regions were consistently found in and right temporal pole and planum polare in patients as compared to healthy controls. In addition, SUV_{COR_norm} detected more asymmetric homologous brain regions than SUV_{WM_norm} and SUV_{global_norm} both in healthy controls and epilepsy patients. We also found that $AI > 10\%$

and SUV ratios > 1.2 were concordant in detecting asymmetry in different brain regions. Therefore, integrated PET/MR can play an important role in the evaluation of epilepsy patients by revealing underlying abnormalities and helping understand their etiopathogenesis.

Interictal ^{18}F -FDG PET typically shows reduced hypometabolism in the epileptogenic region, which can result from a variety of mechanisms, including neuronal loss, diaschisis, reduced synaptic density, or excess inhibition [22]. Cortical hypometabolism may be associated with the duration, frequency, and severity of the seizures [23]. Hippocampal sclerosis is a common etiology in adult epilepsy, which may

explain why the temporal pole and planum polare (anterior portion of the superior surface of the temporal lobe) were two nearby regions that showed significant hypometabolism in the patients compared to healthy controls in our study.

In epilepsy patients, a restricted area of focal hypermetabolism is frequently concordant with surface electroencephalographic (EEG) recording during the ictal PET [24]. This area is suggestive of epileptogenic focus and would show hypometabolism in the interictal PET. However, paradoxical increase in focal cortical glucose metabolism occurs in some epilepsy patients with malformations of cortical development [25], possibly resulting from extremely frequent interictal discharges. Although the hypermetabolism findings in our interictal PET/MR study of epilepsy patients relative to normal controls are atypical, progressive, age-dependent metabolic changes (hyper- as well as hypometabolism) occur in the brain of rats during epileptogenesis [17, 26-28]. Studies of the interictal state in various rat models also found evidence for bilateral hypermetabolism in the amygdala/hippocampal complex [29-31]. Children with transient hypermetabolism had a higher rate of subsequent epilepsy surgery as compared to those without hypermetabolism [17]. Hypermetabolism can also occur shortly after the first clinical seizures in children with Sturge-Weber syndrome [32]. Eiderlberg and his colleagues have suggested that abnormal electrical activity originating in the seizure focus could affect remote areas, which could lead to metabolic abnormalities. In their interictal study, they reported both elevations (hyper-) and depressions (hypo-) of metabolism in TLE patients, as compared to normal controls (Rubin 1995). The hypermetabolism of the postcentral gyrus (primary sensory cortex) and precentral gyrus (primary motor cortex) were observed in our interictal studies. These findings have not been reported previously and are not well understood. To our knowledge, our study is the first to compare epilepsy patients with control in over 117 brain regions. Epilepsy (seizure disorders) has been characterized as clinical or subclinical disturbances of cortical function due to a sudden, abnormal, excessive, and disorganized discharge of brain cells, with clinical manifestations including abnormal motor, sensory and psychic phenomena [33]. Our findings on the metabolic alterations in the

sensory and motor cortex of epilepsy patients are in fact consistent with the neurological manifestations in epilepsy. We hypothesize potential mechanisms: 1) disinhibition of primary sensorimotor regions from compensatory processes originating in other brain regions, 2) subtle malformations of cortical development may be present in sensorimotor regions in some patients, and 3) other unknown processes. However, more studies with large group of patients are necessary to replicate our findings and assess our hypotheses.

To detect subtle abnormalities that are likely to be missed on visual inspection, quantification of radiotracer uptake in different cortical regions is necessary, especially for localization of epileptogenic zones. Several investigations have examined quantitative features of PET in epilepsy patients with varying results [34-41]. Prior studies used labor-intensive methods (e.g., hand-drawn region-of-interest (ROI) analyses) [38-40] or quantitatively analyzed differences in ROIs using a probabilistic atlas based on normal anatomical information [42]. Such atlases estimate the probability that a given voxel in a standard space belongs to a particular region. Probability estimates are based on the proportion of voxels at a given location in a set of individual manually labeled brains registered to the template space that have been assigned any given label [43]. For example, the Harvard-Oxford atlas (distributed with the FSL software package; <http://fsl.fmrib.ox.ac.uk/fsl/>), was created by affine-registering 37 individual scans that were each manually parcellated according to the morphometric analysis [44] to MNI (Montreal Neurological Institute) space using the FLIRT tool in FSL. These voxel-based morphometry analyses provide quantitative assessment of the neocortex in various forms of epilepsy and have the potential to demonstrate subtle abnormalities that are not identified by eye because of anatomic variability [45].

Our quantitative voxel-based analysis of PET activity may add values to visual qualitative analysis. It has replaced manual ROI analysis and has provided tools to make statistical inferences at voxel level [46]. Quantitative analysis can be performed equally well in both left and right hemispheres, whereas visual analysis was more sensitive in detecting left-hemispheric hypometabolism [47]. However, some degree

Study in epilepsy using simultaneous PET/MR

of normal glucose metabolic asymmetry, particularly lower metabolism in the left cortex, is present in the normal human brain [48]. Therefore, the cut-off level of asymmetry is important for determining abnormalities and differentiating patients from healthy subjects. Our results of concordance of AI > 10% and SUV ratios > 1.2 may be helpful to apply these two methods to detect asymmetric glucose metabolism for searching epileptogenic foci in epilepsy patients.

The versatility of MR imaging method, the better soft-tissue contrast and the operation without ionizing radiation may render PET/MR the preferred hybrid imaging technique for many applications [49]. The use of non-invasive PET/MR imaging to identify the epileptic zone could reduce the need for more expensive stereo-EEG investigations, while providing a better diagnostic definition of patients with complex epilepsy. Alternatively, in patients who are not candidates for surgical treatment, the new approach may give insight into the physiological mechanism of drug-resistance or possibly inform the development of innovative treatment strategies [50].

The limitation of our study is that the patients were not homogenous and not age-matched to controls. Besides, in the PET/MR system, an acquisition time of 60 min was chosen to take advantage of the simultaneous acquisition of MR imaging. The optimal time frame for PET acquisition in the PET/MR is a current research subject. Furthermore, confounding clinical issues that may affect global or regional cerebral metabolism - such as the type of seizures, time since the most recent seizure, neuropsychiatric conditions such as depression, and use of anticonvulsants - should be considered in the evaluation of PET scans. The fact that our preliminary results (e.g., abnormal regional glucose metabolism and prevalence of asymmetry) are consistent with the clinical data of epilepsy patients suggests that simultaneous PET/MR imaging provides a useful imaging tool to identify regional abnormality and assist in localizing the seizure focus. Therefore, the results of this study may pave the way for larger prospective PET studies in epilepsy populations. This would also allow further analysis of PET performance in different brain regions, which could not be done in the present study because of the limited sample size.

Conclusion

Our study of interictal metabolic alterations in epilepsy employed: (1) a state-of-the-art integrated PET/MR scanner with simultaneous acquisition, (2) a normal control group as a stable reference for metabolic and asymmetry comparisons, (3) quantitative data analysis methods for over 117 brain regions, (4) statistical analyses on SUV values derived from three normalization methods for comparison to avoid potential sources of variability, (5) direct correlations of FDG uptake with MR regional abnormality. We found both hypermetabolism and hypometabolism regions that were consistently detected by all three normalization methods in the interictal state compared with normal controls. Some of the abnormalities beyond the typically investigated temporal regions were in fact consistent with the clinical manifestations of epilepsy, including abnormal motor and sensory systems.

Taken together, as an innovative and more comprehensive approach to the study of epilepsy, simultaneous PET/MR may play an increasingly important role in the non-invasive evaluation of patients with epilepsy. It can also be used in the evaluation of various epileptic syndromes, particularly those with unknown causes, by revealing some underlying abnormalities, thus helping to understand etiopathogenesis but also to assist in more accurate planning for resective surgery.

Acknowledgements

The authors thank the staff of the Center for Biomedical Imaging at New York University School of Medicine for their technical expertise and support, and the staff of Comprehensive Epilepsy Center for their recruitment and scheduling effort, and Drs. David Faul and Fernando Boada at Radiology for their advice. Funding for this study was provided by the Department of Radiology at New York University School of Medicine.

Disclosure of conflict of interest

None of the authors reports any biomedical financial interests or potential conflicts of interests.

Address correspondence to: Yu-Shin Ding, Departments of Radiology and Psychiatry, New York

Study in epilepsy using simultaneous PET/MR

University School of Medicine, 660 First Avenue, 4th Floor, New York, NY 10016, USA. Tel: 212-263-6605; Fax: 212-263-7541; E-mail: yu-shin.ding@nyumc.org; yushin.ding@nyu.edu

References

- [1] Newberg AB and Alavi A. PET in seizure disorders. *Radiol Clin North Am* 2005; 43: 79-92.
- [2] Dickson JC, O'Meara C and Barnes A. A comparison of CT- and MR-based attenuation correction in neurological PET. *Eur J Nucl Med Mol Imaging* 2014; 41: 1176-89.
- [3] Wurslin C, Schmidt H, Martirosian P, Brendle C, Boss A, Schwenzer NF and Stegger L. Respiratory motion correction in oncologic PET using T1-weighted MR imaging on a simultaneous whole-body PET/MR system. *J Nucl Med* 2013; 54: 464-471.
- [4] Fung EK and Carson RE. Cerebral blood flow with [¹⁵O]water PET studies using an image-derived input function and MR-defined carotid centerlines. *Phys Med Biol* 2013; 58: 1903-1923.
- [5] Xiong J, Nickerson LD, Downs JH 3rd and Fox PT. Basic principles and neurosurgical applications of positron emission tomography. *Neurosurg Clin N Am* 1997; 8: 293-306.
- [6] Diehl B, LaPresto E, Najm I, Raja S, Rona S, Babb T, Ying Z, Bingaman W, Luders HO and Ruggieri P. Neocortical temporal FDG-PET hypometabolism correlates with temporal lobe atrophy in hippocampal sclerosis associated with microscopic cortical dysplasia. *Epilepsia* 2003; 44: 559-564.
- [7] Hermann BP, Lin JJ, Jones JE and Seidenberg M. The emerging architecture of neuropsychological impairment in epilepsy. *Neurol Clin* 2009; 27: 881-907.
- [8] Juhasz C and Chugani HT. Imaging the epileptic brain with positron emission tomography. *Neuroimaging Clin N Am* 2003; 13: 705-716, viii.
- [9] Dukart J, Mueller K, Horstmann A, Vogt B, Frisch S, Barthel H, Becker G, Moller HE, Villringer A, Sabri O and Schroeter ML. Differential effects of global and cerebellar normalization on detection and differentiation of dementia in FDG-PET studies. *Neuroimage* 2010; 49: 1490-1495.
- [10] Newberg AB, Wang J, Rao H, Swanson RL, Wintering N, Karp JS, Alavi A, Greenberg JH and Detre JA. Concurrent CBF and CMRGlc changes during human brain activation by combined fMRI-PET scanning. *Neuroimage* 2005; 28: 500-506.
- [11] Rakheja R, DeMello L, Chandarana H, Glielmi C, Geppert C, Faul D and Friedman KP. Comparison of the accuracy of PET/CT and PET/MRI spatial registration of multiple metastatic lesions. *AJR Am J Roentgenol* 2013; 201: 1120-1123.
- [12] Desikan RS, Segonne F, Fischl B, Quinn BT, Dickerson BC, Blacker D, Buckner RL, Dale AM, Maguire RP, Hyman BT, Albert MS and Killiany RJ. An automated labeling system for subdividing the human cerebral cortex on MRI scans into gyral based regions of interest. *Neuroimage* 2006; 31: 968-980.
- [13] Jeong Y, Song YM, Chung PW, Kim EJ, Kang SJ, Kim JM, Cho SS, Kim SE, Byun HS and Na DL. Correlation of ventricular asymmetry with metabolic asymmetry in frontotemporal dementia. *J Neuroradiol* 2005; 32: 247-254.
- [14] Gaillard WD, Berl MM, Duke ES, Ritzl E, Miranda S, Liew C, Finegersh A, Martinez A, Dustin I, Sato S and Theodore WH. fMRI language dominance and FDG-PET hypometabolism. *Neurology* 2011; 76: 1322-1329.
- [15] Theodore WH, Fishbein D and Dubinsky R. Patterns of cerebral glucose metabolism in patients with partial seizures. *Neurology* 1988; 38: 1201-1206.
- [16] Muzik O, Chugani DC, Shen C, da Silva EA, Shah J, Shah A, Canady A, Watson C and Chugani HT. Objective method for localization of cortical asymmetries using positron emission tomography to aid surgical resection of epileptic foci. *Comput Aided Surg* 1998; 3: 74-82.
- [17] Alkonyi B, Chugani HT and Juhasz C. Transient focal cortical increase of interictal glucose metabolism in Sturge-Weber syndrome: implications for epileptogenesis. *Epilepsia* 2011; 52: 1265-1272.
- [18] Curatolo P, Bombardieri R and Jozwiak S. Tuberculous sclerosis. *Lancet* 2008; 372: 657-668.
- [19] Crino PB, Nathanson KL and Henske EP. The tuberous sclerosis complex. *N Engl J Med* 2006; 355: 1345-1356.
- [20] Bollo RJ, Kalhorn SP, Carlson C, Haegeli V, Devinsky O and Weiner HL. Epilepsy surgery and tuberous sclerosis complex: special considerations. *Neurosurg Focus* 2008; 25: E13.
- [21] Kalantari BN and Salamon N. Neuroimaging of tuberous sclerosis: spectrum of pathologic findings and frontiers in imaging. *AJR Am J Roentgenol* 2008; 190: W304-309.
- [22] Kumar A and Chugani HT. The role of radionuclide imaging in epilepsy, Part 1: Sporadic temporal and extratemporal lobe epilepsy. *J Nucl Med* 2013; 54: 1775-1781.
- [23] Gaillard WD, Kopylev L, Weinstein S, Conry J, Pearl PL, Spanaki MV, Fazilat S, Venzina LG, Dubovsky E and Theodore WH. Low incidence of abnormal (18)FDG-PET in children with new-onset partial epilepsy: a prospective study. *Neurology* 2002; 58: 717-722.

Study in epilepsy using simultaneous PET/MR

- [24] Meltzer CC, Adelson PD, Brenner RP, Crumrine PK, Van Cott A, Schiff DP, Townsend DW and Scheuer ML. Planned ictal FDG PET imaging for localization of extratemporal epileptic foci. *Epilepsia* 2000; 41: 193-200.
- [25] Poduri A, Golja A, Takeoka M, Bourgeois BF, Connolly L and Riviello JJ Jr. Focal cortical malformations can show asymmetrically higher uptake on interictal fluorine-18 fluorodeoxyglucose positron emission tomography (PET). *J Child Neurol* 2007; 22: 232-237.
- [26] Dube C, Boyet S, Marescaux C and Nehlig A. Progressive metabolic changes underlying the chronic reorganization of brain circuits during the silent phase of the lithium-pilocarpine model of epilepsy in the immature and adult Rat. *Exp Neurol* 2000; 162: 146-157.
- [27] Dube C, da Silva Fernandes MJ and Nehlig A. Age-dependent consequences of seizures and the development of temporal lobe epilepsy in the rat. *Dev Neurosci* 2001; 23: 219-223.
- [28] Guo Y, Gao F, Wang S, Ding Y, Zhang H, Wang J and Ding MP. In vivo mapping of temporospatial changes in glucose utilization in rat brain during epileptogenesis: an 18F-fluorodeoxyglucose-small animal positron emission tomography study. *Neuroscience* 2009; 162: 972-979.
- [29] VanLandingham KE and Lothman EW. Self-sustaining limbic status epilepticus. I. Acute and chronic cerebral metabolic studies: limbic hypermetabolism and neocortical hypometabolism. *Neurology* 1991; 41: 1942-1949.
- [30] White LE and Price JL. The functional anatomy of limbic status epilepticus in the rat. I. Patterns of 14C-2-deoxyglucose uptake and Fos immunocytochemistry. *J Neurosci* 1993; 13: 4787-4809.
- [31] Handforth A, Finch DM, Peters R, Tan AM and Treiman DM. Interictal spiking increases 2-deoxy[14C]glucose uptake and c-fos-like reactivity. *Ann Neurol* 1994; 35: 724-731.
- [32] Williams PA, White AM, Clark S, Ferraro DJ, Swiercz W, Staley KJ and Dudek FE. Development of spontaneous recurrent seizures after kainate-induced status epilepticus. *J Neurosci* 2009; 29: 2103-2112.
- [33] Adams RD VM, Ropper AH. Principles of Neurology. Companion Handbook. 6th edition. 1998.
- [34] Ferrie CD, Marsden PK, Maisey MN and Robinson RO. Visual and semiquantitative analysis of cortical FDG-PET scans in childhood epileptic encephalopathies. *J Nucl Med* 1997; 38: 1891-1894.
- [35] Manno EM, Sperling MR, Ding X, Jaggi J, Alavi A, O'Connor MJ and Reivich M. Predictors of outcome after anterior temporal lobectomy: positron emission tomography. *Neurology* 1994; 44: 2331-2336.
- [36] Theodore WH, Sato S, Kufta CV, Gaillard WD and Kelley K. FDG-positron emission tomography and invasive EEG: seizure focus detection and surgical outcome. *Epilepsia* 1997; 38: 81-86.
- [37] Kim YK, Lee DS, Lee SK, Kim SK, Chung CK, Chang KH, Choi KY, Chung JK and Lee MC. Differential features of metabolic abnormalities between medial and lateral temporal lobe epilepsy: quantitative analysis of (18)F-FDG PET using SPM. *J Nucl Med* 2003; 44: 1006-1012.
- [38] Lee DS, Lee JS, Kang KW, Jang MJ, Lee SK, Chung JK and Lee MC. Disparity of perfusion and glucose metabolism of epileptogenic zones in temporal lobe epilepsy demonstrated by SPM/SPAM analysis on 15O water PET, [18F]FDG-PET, and [99mTc]-HMPAO SPECT. *Epilepsia* 2001; 42: 1515-1522.
- [39] Wong CY, Geller EB, Chen EQ, MacIntyre WJ, Morris HH 3rd, Raja S, Saha GB, Luders HO, Cook SA and Go RT. Outcome of temporal lobe epilepsy surgery predicted by statistical parametric PET imaging. *J Nucl Med* 1996; 37: 1094-1100.
- [40] Hikima A, Mochizuki H, Oriuchi N, Endo K and Morikawa A. Semiquantitative analysis of interictal glucose metabolism between generalized epilepsy and localization related epilepsy. *Ann Nucl Med* 2004; 18: 579-584.
- [41] Muzik O, Pourabdollah S, Juhasz C, Chugani DC, Janisse J and Draghici S. Application of an objective method for localizing bilateral cortical FDG PET abnormalities to guide the resection of epileptic foci. *IEEE Trans Biomed Eng* 2005; 52: 1574-1581.
- [42] Lee SK, Lee DS, Yeo JS, Lee JS, Kim YK, Jang MJ, Kim KK, Kim SK, Oh JB and Chung CK. FDG-PET images quantified by probabilistic atlas of brain and surgical prognosis of temporal lobe epilepsy. *Epilepsia* 2002; 43: 1032-1038.
- [43] Bohland JW, Bokil H, Allen CB and Mitra PP. The brain atlas concordance problem: quantitative comparison of anatomical parcellations. *PLoS One* 2009; 4: e7200.
- [44] Caviness VS Jr, Meyer J, Makris N and Kennedy DN. MRI-Based Topographic Parcellation of Human Neocortex: An Anatomically Specified Method with Estimate of Reliability. *J Cogn Neurosci* 1996; 8: 566-587.
- [45] Bernasconi A. Quantitative MR imaging of the neocortex. *Neuroimaging Clin N Am* 2004; 14: 425-436, viii.
- [46] Astrakas LG and Argyropoulou MI. Shifting from region of interest (ROI) to voxel-based analysis in human brain mapping. *Pediatr Radiol* 2010; 40: 1857-1867.
- [47] Kumar A, Juhasz C, Asano E, Sood S, Muzik O and Chugani HT. Objective detection of epileptic foci by 18F-FDG PET in children undergoing

Study in epilepsy using simultaneous PET/MR

- epilepsy surgery. *J Nucl Med* 2010; 51: 1901-1907.
- [48] Kang E, Lee DS, Kang H, Lee JS, Oh SH, Lee MC and Kim CS. Age-associated changes of cerebral glucose metabolic activity in both male and female deaf children: parametric analysis using objective volume of interest and voxel-based mapping. *Neuroimage* 2004; 22: 1543-1553.
- [49] Schwenzer NF, Stegger L, Bisdas S, Schraml C, Kolb A, Boss A, Muller M, Reimold M, Erne-
mann U, Claussen CD, Pfannenbergl C and Schmidt H. Simultaneous PET/MR imaging in a human brain PET/MR system in 50 patients-
current state of image quality. *Eur J Radiol* 2012; 81: 3472-3478.
- [50] Storti SF, Boscolo Galazzo I, Del Felice A, Pizzini FB, Arcaro C, Formaggio E, Mai R and Mangano P. Combining ESI, ASL and PET for quantitative assessment of drug-resistant focal epilepsy. *Neuroimage* 2013; [Epub ahead of print].